Development 140, 2933-2941 (2013) doi:10.1242/dev.088286

Neuropilin-1 biases dendrite polarization in the retina

Elizabeth M. Kita, Gabriel E. Bertolesi, Carrie L. Hehr, Jillian Johnston and Sarah McFarlane*

SUMMARY

The majority of neurons in the nervous system exhibit a polarized morphology, with multiple short dendrites and a single long axon. It is clear that multiple factors govern polarization in developing neurons, and the biased accumulation of intrinsic determinants to one side of the cell, coupled with responses to asymmetrically localized extrinsic factors, appears to be crucial. A number of intrinsic factors have been identified, but surprisingly little is known about the identity of the extrinsic signals. Here, we show *in vivo* that neuropilin-1 (Nrp1) and its co-receptor plexinA1 (Plxna1) are necessary to bias the extension of the dendrites of retinal ganglion cells to the apical side of the cell, and ectopically expressed class III semaphorins (Sema3s) disrupt this process. Importantly, the requirement for Nrp1 and Plxna1 in dendrite polarization occurs at a developmental time point after the cells have already extended their basally directed axon. Thus, we propose a novel mechanism whereby an extrinsic factor, probably a Sema3, acts through Nrp1 and Plxna1 to promote the asymmetric outgrowth of dendrites independently of axon polarization.

KEY WORDS: Semaphorin, Retinal ganglion cell, *Xenopus*, Plexin

INTRODUCTION

Neurons are polarized structures, generally with a single, long axon and an arbor of short, branched dendrites, present on opposite sides of the cell. Polarization is crucial for neuronal function and is necessary for the emergence of working networks in the brain. How a neuron acquires this polarized form has been studied *in vitro* using the hippocampal neuron culture model (Arimura and Kaibuchi, 2007; Barnes and Polleux, 2009; Tahirovic and Bradke, 2009). In the uniform extracellular milieu of the culture dish, several intrinsic mechanisms have been identified that break symmetry of the initially non-polarized cells, allowing an axon to develop from one of several existing neurites, and dendrites from the remainder. *In vivo*, however, intrinsic determinants are likely to work in tandem with extracellular factors to break symmetry (Barnes and Polleux, 2009). However, the identities of the extrinsic signals responsible for the development of neuronal polarity, and those that control dendrite polarization in particular, remain largely unresolved.

In some neurons, axonal and dendrite polarization appear to be linked. For example, the dendrites of *Xenopus* spinal cord interneurons emerge from the proximal axon (Nishiyama et al., 2011), whereas for cultured mouse hippocampal neurons, dendrite polarization probably occurs secondary to the inhibition of axon initiation (Shelly et al., 2011). Polarization of the axon and dendrites of the retinal ganglion cell (RGC), however, appears to occur independently. For instance, axon but not dendrite orientation requires the lamina of the basal retinal surface (Choi et al., 2010). Thus, the RGC serves as a useful model neuron in which certain aspects of dendrite polarization can be investigated independently of axon development. We took advantage of the experimental amenability of the RGC of *Xenopus laevis* (McFarlane and Lom, 2012) to explore extrinsic factor regulation of dendrite polarization *in vivo*.

Although several factors can induce polarization *in vitro* (Barnes and Polleux, 2009), the current list of participating molecules *in vivo* is relatively limited. A member of the class III family of secreted semaphorins (Sema3s), Sema3a, is one of only a few shown to polarize cells *in vivo* (Nishiyama et al., 2011; Shelly et al., 2011). Sema3s are thought to act through a holoreceptor of a neuropilin (Nrp) and a plexin (Plxn) receptor; the Nrp binds Sema3 and the Plxn transduces the signal into the cell (Zhou et al., 2008). Sema3s impact the growth of dendrites of various neuron types (Gonthier et al., 2009; Kim and Chiba, 2004; Koncina et al., 2007; Morita et al., 2006; Polleux et al., 2000; Schlomann et al., 2009). For cortical neurons, Sema3a is particularly relevant as it promotes the growth of dendrites of cultured mouse hippocampal neurons by suppressing axon initiation and extension (Shelly et al., 2011), and *in vivo* it first aids polarization of mouse cortical pyramidal neurons (Shelly et al., 2011), and later repels axons and attracts dendrites (Polleux et al., 2000).

Xenopus RGCs initiate an axon shortly after they are born, with dendrites emerging only once the axon has entered the brain (Holt, 1989). It is at this point that *Xenopus* RGCs initiate expression of Nrp1 and Plxna1, equipping their axons with the ability to respond to Sema3a as a repellent both *in vitro* and *in vivo* (Atkinson-Leadbeater et al., 2010; Campbell et al., 2001). Intriguingly, a number of Sema3 genes are expressed in the retina after the majority of RGC axons have left the eye and the dendrites start to emerge (Callander et al., 2007; Koestner et al., 2008). As such, we investigated whether Nrp and PlxnA receptors regulate the growth of RGC dendrites *in vivo*.

We report that *sema3a* and *sema3f* are expressed to the basal and apical side of the *Xenopus* RGC, respectively. Impairing the function of the Nrp1-Plxna1 receptors, which are known to transduce Sema3 signals, prevents the biased orientation of dendrites to the apical side of the RGC, a phenotype also generated when Sema3 signals in the retina are disrupted. These data identify Nrp1 and Plxna1 as co-receptors of an extrinsic cue, probably a Sema3, which provides orientation information to developing RGCs for their proper polarization.

MATERIALS AND METHODS

Animals

Xenopus laevis oocytes were produced by adult females primed using human chorionic gonadotrophin (Chorulon, Intervet). Embryos were raised

Hotchkiss Brain Institute, Department of Cell Biology and Anatomy, University of Calgary, 3330 Hospital Drive, Calgary, AB T2N 4N1, Canada.

*Author for correspondence (smcfarla@ucalgary.ca)

Accepted 8 May 2013

in 0.1× Marc's Modified Ringer's solution (MMR; 0.1 M NaCl, 2 mM KCl, 1 mM $MgCl_2$, 5 mM HEPES, pH 7.5) at 16-25°C, and staged according to Nieuwkoop and Faber (Nieuwkoop and Faber, 1994).

Cloning of *Xenopus* full-length *plxn* and *nrp*

The human amino acid sequences of individual Sema3 genes, *PLXNA1*, *NRP1* and *NRP2* were blasted against *Xenopus laevis* expressed sequence tag (EST) sequences (six open reading frames) in the Xenbase and NIH databases. Full-length sequence for *sema3a* (NM_001085855), *sema3c* (NM_001094933), *sema3d* (NM_001094120.1), *sema3f* (NM_001127791.1), *plxna1* (NM_001094988), *nrp1* (NM_001087911.1) and *nrp2* (NM_001091238) were identified. Full-length coding sequence of each *sema3* gene was amplified by RT-PCR of cDNA obtained from stage 37/38 embryos. *nrp1* and *nrp2* were amplified from IMAGE clones obtained from Open Biosystems (clones 4964968 and 5572834, respectively).

Expression constructs and oligonucleotides

Full-length products were cloned into either pCRII-TOPO (Invitrogen) or p-JET (Fermentas, Canada) vectors, and then subcloned into *pCS2-mt* or *pCS2-mtc2* vectors, inserting myc tags (mt) in-frame at the carboxy-terminus of the protein. The expression constructs are named *CS2-sema3a-mt*, *CS2-sema3c-mt*, *CS2-sema3d-mt* and *CS2-sema3f-mt*. A dominant-negative (dn) *nrp1* (*dnnrp1*) construct was engineered as described by Renzi et al. (Renzi et al., 1999), whereby the sequence encoding the MAM domain (nucleotide 1907 to 2372) was deleted. The sequences encoding the 5′ end (nucleotides 1-1906) and 3′ end (nucleotides 2372-2817) were amplified from the IMAGE clone and inserted into the *pCS2-mtc2* expression vector in frame with a myc tag. Phosphorothioate modified oligonucleotides were synthesized based on the mRNA sequences for antisense (AS)-*sema3f* (GCCAATGAATAATCAGGGGTTCC) and sense *sema3a* (NM_001085855.1: nt 209-231).

RNA *in situ* hybridization

Antisense riboprobes were synthesized from linearized cDNA templates using SP6 or T7 RNA polymerases (Roche) and digoxigenin- (DIG) labeled nucleotides (Roche), and stored at −80°C. Embryos were fixed in 4% MEMFA [0.1 M MOPS (3-[N-morpholino] propanesulfonic acid), 2 mM EGTA (ethylene glycol tetraacetic acid), 1 mM MgSO4, 4% formaldehyde in diethylpyrocarbonate-treated H_2O] and stored at −20°C in ethanol. Whole-mount RNA *in situ* hybridization was performed as described previously (Sive et al., 2000). For analysis, embryos were rehydrated, permeabilized with proteinase K, pre-hybridized for 4 hours at 60°C, and hybridized with probe overnight at 60°C. After washing, embryos were incubated in a 1:2000 dilution of anti-DIG antibody (Roche) conjugated to alkaline phosphatase at 4°C. BM Purple (Roche) was used to develop the staining. After fixing in Bouin's solution and bleaching, embryos were stored in TBS and EDTA.

For slide *in situ* hybridization, 12-μm transverse sections of embryos embedded in optimal cutting temperature compound (OCT; Tissue-Tek) were made with a cryostat. Slides were incubated overnight in hybridization buffer and antisense riboprobe, washed, and anti-DIG (1:2500; Roche) conjugated to alkaline phosphatase added. The staining process used 5-bromo-4-chloro-3-indolyl phosphate (BCIP; Roche) and Nitro Blue tetrazolium chloride (NBT; Roche) substrates in an NTMT solution (100 mM NaCl, 100 mM Tris-HCl pH 9.5, 50 mM $MgCl_2$, 1% Tween 20). Here, and elsewhere in this study, digital images were obtained with Axiovision software and adjusted for brightness and contrast by using Adobe Photoshop CS5.

Sema3-conditioned medium

COS-7 cell lines were maintained in Dulbecco's Modified Eagle's Medium (DMEM; Sigma) plus 0.02% glutamine supplemented with 10% fetal bovine serum (FBS; Invitrogen), and grown in a humidified 5% CO_2: 95% air atmosphere at 37°C. Transient transfection with individual *sema3* constructs was carried out (as per manufacturer's instructions) on 70-80% confluent monolayers in 60-mm dishes with Lipofectamine 2000 (Invitrogen). An empty CS2 vector served as control. Cells were grown for 24 hours in DMEM with 10% fetal calf serum. Conditioned medium was obtained after 24 hours, and centrifuged and filtered through a 22-μm pore filter (Pall Corporation). The presence of each Sema3 in individual conditioned media was confirmed by western blot analysis with anti-myc antibodies (Covance); comparable levels of each Sema3 were present across the various media.

Retinal cell cultures

Eyebuds were dissected from anesthetized stage 32 embryos in 60% L15 (Invitrogen) supplemented with 0.4 mg/ml tricaine methanesulfonate (methanesulfonate salt, Research Organics). Eyebuds were dissociated by incubation in media lacking Ca^{2+} and dissociated cells plated onto coverslips coated with poly-L-ornithine (Sigma-Aldrich) and 10 μg/ml laminin (Sigma Aldrich). Cultures were grown at room temperature in a 1:4 mixture of conditioned media to 2 ml 60% L15 (Invitrogen) with 0.01% bovine serum albumin (BSA) and 1% antibiotic/antimycotic (Invitrogen). Cells were left for 24 hours and then fixed in 2% paraformaldehyde (PFA). Neurofilament associated antigen (NAA) (3A10, Developmental Studies Hybridoma Bank, 1:100) immunoreactivity identified RGCs and their axons, and a β-III-tubulin antibody (Abcam, 1:50) was used to reveal the entire cellular morphology (Hocking et al., 2008). Dendrite analysis was performed with the experimenter blind to the experimental condition. Cells with bright NAA immunoreactivity and at least one axon were included in the analysis. Each RGC was digitally photographed by using a 60× objective and SPOT advanced software. The numbers of primary dendrites and dendrite branch points were recorded, and the lengths of branches were measured using SPOT advanced measurement tools.

Immunostaining

Immunohistochemistry of transverse cryostat sections was performed using previously published methods (McFarlane et al., 1995). Primary antibodies included anti-Sema3a (Abcam, 1:1500), anti-neuropilin-1 (C19, Santa Cruz Technologies, 1:100), anti-myc mouse monoclonal 9E10 (Abcam, 1:500) and rabbit anti-vsv (GenScript, 1:2000). The anti-Sema3a antibody recognized a band of the appropriate size in a western blot of protein extract from COS-7 cells transfected with *Xenopus sema3a-mt* (data not shown). For Sema3a and Nrp1 antibody labeling, an intermediate amplification step was performed. Alexa Fluor 488 (1:1000, Molecular Probes), Alexa Fluor 546 (1:1000, Molecular Probes) and Cy3 (1:500, Jackson ImmunoResearch) secondary antibodies were used.

Electroporation

Electroporation was performed as described previously (Hocking et al., 2010). A Picospritzer II was used to make repeated injections of a 0.25-1 μg/ml DNA or RNA mixture through a borosilicate glass needle medial to the eye primordium of stage 27/28 embryos. *CS2-gfp* was electroporated alone as a control. Experiments included co-electroporation of *CS2-gfp* with: (1) either *CS2-dnnrp1-mt* or human *pcDNA3-dnplxna1-vsv* (Tamagnone et al., 1999), (2) either *CS2-sema3a-mt*, *CS2-sema3d-mt*, *CS2-sema3f-mt* or *CS2-caplxna1-mt* [caplxna1 is a constitutively active form of Plxna1 (*plexinA1Δect*) (Takahashi and Strittmatter, 2001)], and (3) either an antisense *sema3f* oligonucleotide (AS-*sema3f*) or a sense *sema3a* oligonucleotide. Embryos developed at room temperature in 0.1× MMR until stage 39/40 were fixed overnight in 4% PFA, and processed for section immunohistochemistry with either an anti-myc or an anti-vsv antibody. A line parallel to the vitreal surface of the retina was used to divide cells into apical and basal retinal halves. Cells for which assignment of neurites into either compartment was ambiguous were removed from the analyses (<5% of cells).

Statistical analysis

For the culture experiments, to account for the small number of data points (*N*=number of independent experiments), an arcsine transformation was used to normalize percentage data (Sokal and Rohlf, 2011), and a square-root transformation for data counts. A one-way ANOVA was performed, and where differences between means were detected, pairwise comparisons were performed using a Dunnett's multiple comparison test. For the *in vivo* dendrite analysis, comparisons between two groups were made using a two-tailed Mann–Whitney U test or Student's *t*-test, and between multiple groups with a non-parametric Kruskal–Wallis test, followed by pairwise

comparisons using a Dunn's multiple comparison test. All statistical tests were applied using GraphPad Prism 4.0 software.

RESULTS

Nrp1 and Plxna1 receptors and Sema3 ligands are expressed in the retina as RGC dendrites emerge

Sema3s bind an Nrp co-receptor to transduce a signal through Plxna1-4 (Zhou et al., 2008). To investigate the involvement of Sema3 in RGC dendritogenesis we examined the retinal expression of *nrp1*, *nrp2* and *plxna1*, and potential Sema3 ligands for these receptors, *sema3a*, *sema3c*, *sema3d* and *sema3f*. Of note, *sema3e* is not expressed in the developing eye (S. Meadows, personal communication). We performed RNA *in situ* hybridization of transverse sections of *Xenopus* retina, spanning the period from dendrite initiation (stage 32) to the establishment of a primitive arbor at stage 40 (Holt, 1989).

The expression patterns of *nrp1*, *plxna1* and several Sema3 genes suggest potential roles in RGC dendrite development. *sema3a* mRNA (Fig. 1A,G) and protein are present in the lens (stage 32) and in the photoreceptors of the outer nuclear layer (stage 33/34), with expression maintained at least until stage 40 (Fig. 1L). From stage 32 to stage 40, *sema3d* is expressed in the proliferative ciliary marginal zone of the peripheral retina (Fig. 1C,H). Finally, *sema3f* turns on in cells of the inner nuclear layer, which are likely to be the synaptic partners of the emerging RGC dendrites (Fig. 1D,I). mRNA is present throughout the period of RGC dendritogenesis. Nrp1 and Plxna1 receptors are known to be present in RGCs from stage 35/36 onwards (Campbell et al., 2001; Ohta et al., 1992; Takagi et al., 1991), and we find that *nrp1* and *plxna1* transcripts are present as early as stage 32 (Fig. 1E,F,J,K). Further, an antibody that recognizes *Xenopus* neuropilin-1 (Togashi et al., 2008) labels both the axons and dendrites of RGCs in culture and *in vivo* (supplementary material Fig. S1). Of note, *sema3c* (Fig. 1B) and *nrp2* (data not shown) are not expressed as RGC dendrites first extend. In summary, *nrp1* and *plxna1* are expressed in the RGCs, and Sema3 genes in the flanking tissues, suggesting that these receptors could transduce signals to control RGC morphogenesis.

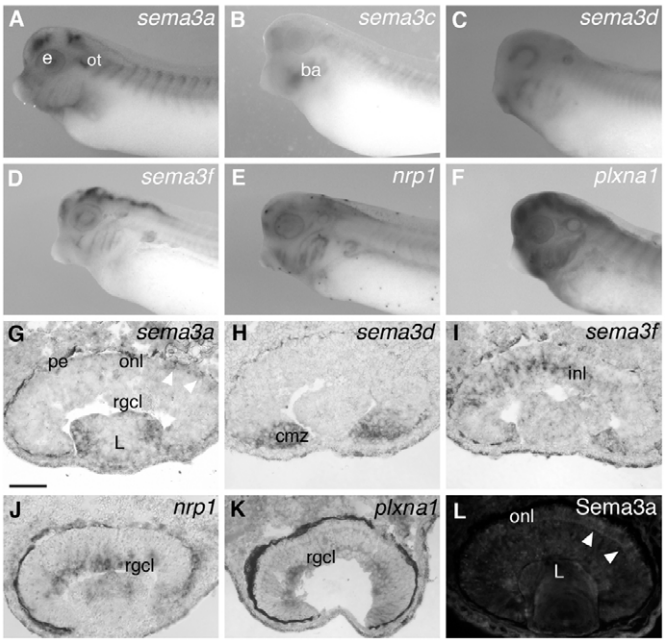

Fig. 1. *nrp1* and *plxna1*, and their *sema3* ligands, expressed in the *Xenopus* retina over the initial period of RGC dendritogenesis. (**A-F**) Lateral views of whole-mount embryos after RNA *in situ* hybridization with *sema3*, *nrp1* and *plxna1* antisense riboprobes at stage 35/36. (**G-K**) Transverse sections through the retina of stage 31/32 (G-I) and stage 35/36 (J,K) embryos with *in situ* hybridization performed directly on the tissue sections. (**L**) Immunolabeling of a stage 37/38 retinal section with an anti-Sema3a antibody. Arrowheads in G and L point to label for *sema3a* mRNA and protein, respectively. ba, branchial arches; cmz, ciliary marginal zone; e, eye; inl, inner nuclear layer; L, lens; onl, outer nuclear layer; ot, otic vesicle; pe, pigment epithelium; rgcl, retinal ganglion cell layer. Scale bar: in G, 50 μm for G-L.

Nrp1 and Plxna1 are required for RGC dendrite polarization *in vivo*

The retina neuroepithelium is polarized, with the pigment epithelium side designated as apical and the vitreal surface next to the lens as basal (Randlett et al., 2011). The RGC axon (Fig. 2A, arrow) emerges from the basal cell surface and projects towards the lens and along the vitreal surface of the retina, whereas the dendrites (Fig. 2A, arrowheads) extend from the apical surface towards the inner plexiform layer. Because RGCs initiating their first dendrites express the Sema3 receptor Nrp1 (Fig. 1; supplementary material Fig S1), we tested the necessity of Nrp1 in RGC dendritogenesis using a dominant-negative mutant *Xenopus* Nrp1 (dnnrp1) we generated based on a chick dnnrp1 (Renzi et al., 1999). The engineered dnnrp1 should bind Sema3s but not Plxns, and thus is unable to transmit a signal (Nakamura and Goshima, 2002; Renzi et al., 1999). A construct encoding a myc-tagged version of dnnrp1, *CS2-dnnrp1-mt*, was electroporated, along with *CS2-gfp*, into stage 28 eye primordia (Hocking et al., 2010) (Fig. 2B), when the first RGCs initiate axons (Holt, 1989). We aimed for low transfection efficiencies, so that the morphology of a transfected RGC in the central retina could be viewed in isolation of neighboring transfected cells. Embryos were left to develop until stage 39, when most RGCs exhibit simple dendritic arbors. The morphology of the transfected cells was visualized by myc immunoreactivity and GFP epifluorescence in transverse retinal sections. *CS2-gfp* here, and throughout our study, served as the control and was used to label the entire RGC and its neurites. Based on the comparison of the myc immunolabeling and the GFP fluorescence, it may be concluded that the dnnrp1 protein is expressed throughout the cell (Fig. 2E).

The majority of control GFP-expressing RGCs (89.9%, n=94 cells) polarize along the apicobasal axis: extending a single axon from the basal cell surface, and one or more dendrite-like processes from the apical surface (Fig. 2C,C′). By contrast, dnnrp1-expressing RGCs often display several basally directed neurites (Fig. 2D,D′), with fewer than half exhibiting a single basally directed neurite (47.2%, n=106 cells). Normally, the emerging basal axon is thin and unbranched, whereas these basal neurites are short, thick and sometimes branched, and thus are likely to represent mislocalized dendrites. Although positive dendrite markers, such as MAP2, are not specific to the RGC dendrites at early stages, we do find that SMI-31, which effectively labels embryonic *Xenopus* RGC axons but not their dendrites (Hocking et al., 2008), labels processes identified as axons by our criteria, but not the short, basal neurites (Fig. 2F-H). Nonetheless, in our quantification we avoided the possibility of mis-identification of the axon and dendrites by calling all processes neurites.

To quantify the effects of the dnnrp1 on RGC dendrite polarity, we assessed the number of basal and apical neurites per cell (Fig. 2K). The dnnrp-expressing cells exhibit significantly more neurites than do control cells [GFP (control), 3.1±0.1 (s.e.m.)

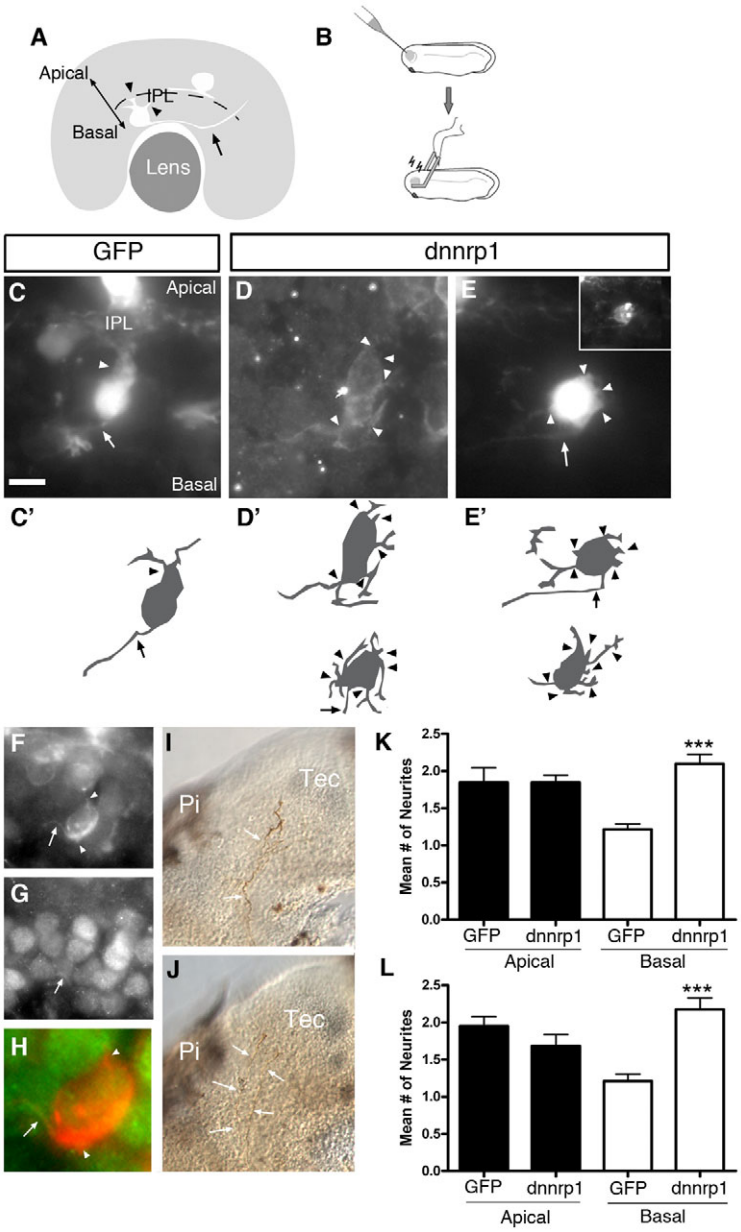

Fig. 2. Inhibiting Sema3 signaling in RGCs disrupts dendrite polarization. (**A**) Schematic of the stage 39 retina. The apical and basal surfaces are labeled, and shown are a representative RGC and amacrine cell, basal and apical to the inner plexiform layer (IPL), respectively. (**B**) Schematic of the electroporation method. (**C-J**) Eyes were electroporated at stage 28 with *CS2-GFP* alone (C,I), or with *CS2-GFP* and *CS2-dnnrp1-mt* (D,E,F-H,J). (C-E) Cells were visualized in sections by GFP epifluorescence (C,E) and/or by 9E10 immunoreactivity for the myc-tag (D, inset in panel E). A control GFP-expressing RGC (C) sends a thin axon down towards the vitreal surface (basal) and dendrites to the IPL. A stage 39 (D) and a stage 42 (E) dnnrp1-expressing RGC both exhibiting an unbiased morphology, with neurites extending from both apical and basal cell surfaces. Images are oriented with basal down and apical up. Axons are indicated with arrows, and dendrite-like neurites with arrowheads. Schematic drawings of the RGCs in C-E, along with additional examples, to capture the scope of phenotypes, are shown in C′-E′. (F-H) Immunolabeling of a dnnrp1-mt-expressing RGC with a myc antibody (F) and the axonal marker SMI-31 (G). Merge is shown at higher magnification in H. SMI-31 labels the axon (arrow) of the RGC but not a short, basal neurite or an apical dendrite (arrowheads). (I,J) GFP- (I) and dnnrp1- (J) expressing RGC axons visualized at stage 40 in a lateral view of a whole-mount brain by immunostaining with an anti-GFP (I) or an anti-myc (J) antibody, respectively. Pi, pineal gland; Tec, optic tectum. Scale bar: in C, 10 μm for C-E,F,G; in C, 5 μm for H. (**K**,**L**) Graphs of the mean number of apical and basal neurites of RGCs expressing dnnrp1 at stage 39 (K) and stage 42 (L). Errors bars represent s.e.m. For K, GFP n=94, dnnrp1 n=106; for L, GFP n=42, dnnrp1 n=57. Data was obtained from at least three independent data replicates. Groups were compared statistically using a two-tailed Mann–Whitney U non-parametric test (***P<0.001).

neurites/cell, n=94; dnnrp1, 4.2±0.1 neurites/cell, n=106 cells; P<0.001, unpaired Student's t-test], because of a significant increase in the number of basal neurites (Fig. 2K). We thus conclude that Nrp1 functions to limit the emergence of neurites to the apical surface of the RGC.

Static analysis of early *Xenopus* RGC morphogenesis suggests that after initiating an axon, RGCs put out a few basal neurites, which are generally lost over hours (Holt, 1989). Thus, the failure of dnnrp1-positive RGCs to acquire a polarized morphology could reflect developmental delay. Our data, however, indicate that even early on at stage 33/34, a day earlier than the stage used for the *in vivo* analyses, the number of basal [1.1±0.05 (s.e.m.), n=67] versus apical (1.5±0.1) processes for wild-type GFP-expressing RGCs shows an apical bias. Nonetheless, to address whether the lack of a clear apical bias of dnnrp-expressing RGCs reflects developmental delay, we left electroporated embryos for another day before assessing the morphology of control GFP- and dnnrp1-expressing RGCs. Older dnnrp1-expressing RGCs (stage 42) still exhibit significantly more neurites than do control RGCs, as a result of higher numbers of basally directed neurites (Fig. 2E,E′,L). Indeed, in contrast to control (19%, n=42), a significant proportion of dnnrp1-expressing RGCs (71.9%, n=57) still display more than one basal neurite at stage 42. These data argue against the dnnrp1-positive RGCs being delayed in their development. In agreement, dnnrp1-positive RGC axons are found in the optic tectum, the major midbrain target, at a developmentally appropriate time point (stage 40; Fig. 2I,J).

Nrp1 functions with a Plxn to mediate Sema3 signaling (Tamagnone et al., 1999). Thus, we postulated that if Sema3 signaling is important in RGC dendrite polarization, blockade of the relevant Plxn should phenocopy the defects in polarization seen with the dnnrp1. Plxna1 protein and mRNA are expressed by stage 35/36 RGCs (Fig. 1F,K) (Ohta et al., 1992). We used a previously characterized truncated human PLXNA1 (dnplxna1), which can block growth cone collapse of *Xenopus* spinal neurons (Tamagnone et al., 1999), to impair Sema3 signaling in RGCs. mRNA for a vsv-tagged *dnplxna1* was electroporated into stage 28 eye primordia; mRNA was necessary in this case to increase the efficiency of

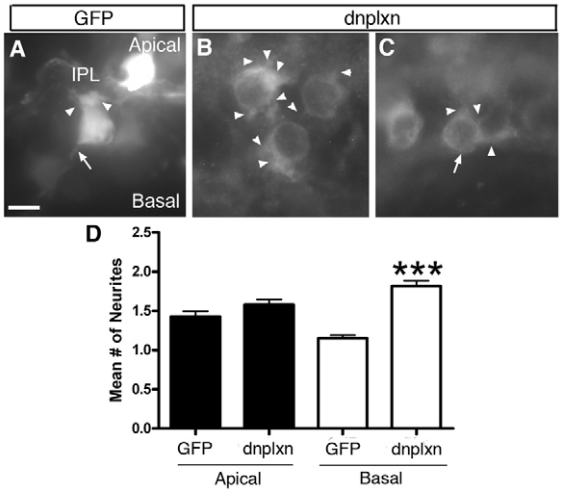

Fig. 3. Blockade of Plxna1 signaling in RGCs disrupts dendrite polarization. (**A-C**) Stage 39 RGCs electroporated at stage 28 with mRNA encoding *GFP* (A), or *GFP* and *dnplxna1* (B,C) were visualized in retinal sections by GFP epifluorescence (A) and/or by immunoreactivity for the vsv-tag (B,C). A control GFP-expressing RGC has a polarized morphology, with dendrites extending towards the inner plexiform layer (IPL), whereas RGCs expressing a truncated Plxna1 receptor have neurites that extend from both apical and basal surfaces of the cell. Images are oriented with basal down and apical up. Axons are indicated with arrows, and dendrite-like neurites with arrowheads. Scale bar: 10 µm. (**D**) Graph of the mean number of apical and basal neurites of RGCs expressing either GFP and/or dnplxn1 at stage 39. Errors bars represent s.e.m. GFP n=151, dnplxna1 n=189. Data was obtained from at least three independent data replicates. Groups were compared statistically using a two-tailed Mann–Whitney U non-parametric test (***P<0.001).

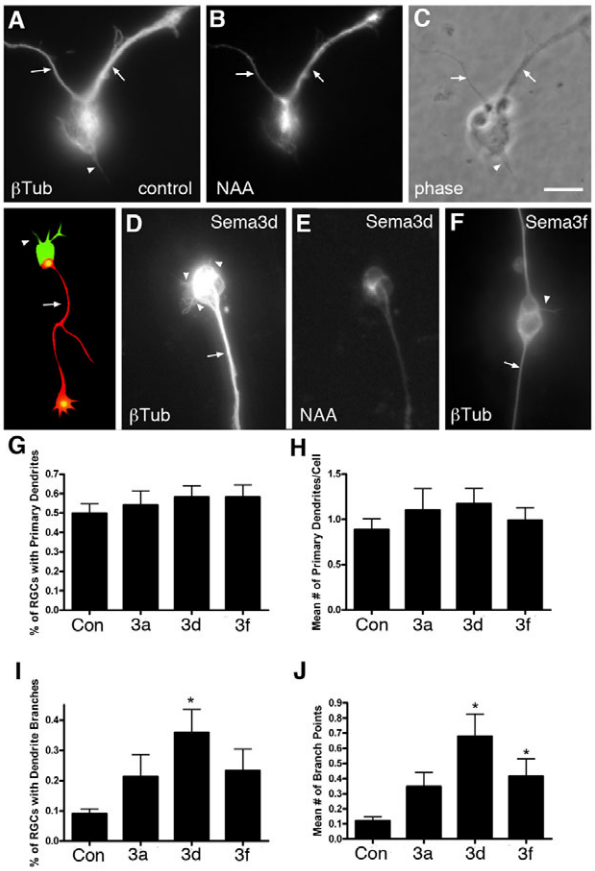

Fig. 4. Sema3s can act directly on RGCs to impact dendritogenesis. (**A-F**) Eye primordia were dissected and dissociated at stage 32, and incubated for 24 hours with conditioned media from COS-7 cells transfected with empty vector as control (A-C), or with transgenes encoding Sema3a, Sema3d (D,E) or Sema3f (F). RGCs were identified by immunolabeling with an antibody that recognizes neurofilament associated antigen (NAA). As seen in the schematic (left), the morphology of the entire cell is revealed with a β-III-tubulin antibody (green), and dendrites (arrowheads) identified as short β-III-tubulin positive processes, showing little or no immunoreactivity with the NAA antibody. By contrast, the axon (arrows) is both β-III-tubulin and NAA positive. Displayed is the β-III-tubulin (A) and NAA (B) immunoreactivity for the control cell shown in phase contrast in C. The β-III-tubulin (D,F) and NAA (E) immunoreactivity for a Sema3d- (D,E) and a Sema3f- (F) exposed cell are presented. Scale bar: 10 µm. (**G-J**) Graphs showing quantification of the percentage of RGCs with primary dendrites (G), the mean number of primary dendrites/cell (H), the percentage of RGCs with dendrites that branch (I) and the mean number of dendrite branch points (J). Error bars represent s.e.m. N=5-7 independent experiments, with 20-50 RGCs assessed for each condition per experiment. Statistical differences between the groups were assessed by using a one-way ANOVA and a Dunnett's post-hoc test (*P<0.05).

transfection. The morphology of dnplxna1-expressing RGCs was assessed at stage 39 by immunolabeling for the vsv tag (Fig. 3B,C). Similar to what is observed for RGCs that express dnnrp1, dnplxna1-positive RGCs exhibit significantly more neurites than do control cells [GFP, 2.56±0.08 (s.e.m.) neurites, n=159; dnplxna1, 3.39±0.09 neurites, n=181; P<0.001, unpaired, two-tailed Student's t-test]. Moreover, they fail to acquire a mature, polarized morphology: the majority of RGCs (56.9%, n=181) display multiple basal dendrite-like neurites, in contrast to control (17%, n=159). Finally, although dnplxna1-expressing RGCs extend comparable numbers of apical neurites to control RGCs, they exhibit significantly more basal neurites (Fig. 3D). Thus, Plxna1 and Nrp1 are likely to combine to bias neurite emergence to the apical surface of the RGC.

Sema3s disrupt RGC dendrite polarization

We find transcripts for the Sema3 receptors in RGCs and for the Sema3 ligands in adjacent cell types, after many RGC axons have left the eye and dendrites are initiating (Holt, 1989), raising the possibility that Nrp1 and Plxna1 transduce a Sema3 within the retina to control RGC dendritogenesis. As such, we first investigated whether Sema3s could act directly on an isolated RGC to impact dendrite development. We exposed isolated RGCs in low-density mixed retinal cultures to different Sema3 proteins *in vitro*. Eye buds were dissected at stage 32, as the first RGC dendrites initiate (Holt, 1989), and plated as dissociated cells for 24 hours in the presence of Sema3-containing conditioned media from transfected COS-7 cells. Immunocytochemistry with an antibody against neurofilament associated antigen (NAA) was used to identify isolated RGCs and their axons, whereas dendrites were characterized as having little or no NAA immunoreactivity (Hocking et al., 2008) (Fig. 4, schematic; supplementary material Fig. S1). This approach can reliably identify RGC axons and dendrites in the absence, to date, of a positive dendrite marker that works in these early stage cultures. Immunolabeling with a β-III-tubulin antibody revealed the full morphology of the RGCs, and helped in visualizing the NAA-negative dendrites. Of note, cultured stage 32 RGCs exhibit both axons and dendrites, yet cells are not polarized as they are *in vivo*, with dendrites present on the opposite side of the cell to the axon.

Instead, dendrites are distributed in no particular relation to the axon (data not shown).

Although Sema3a inhibits the growth of cultured hippocampal axons (Shelly et al., 2011), we observe that axons in Sema3-treated cultures are of similar length to those in control [control, 236.7±18.4 μm (s.e.m.), *n*=7; Sema3a, 275.7±41 μm, *n*=5; Sema3d, 217±30 μm, *n*=7; Sema3f, 267.3±18.2 μm, *n*=6]. Similarly, uniform application of Sema3s has no effect on the mean percentage of RGCs that extend one or more primary dendrites or on the average number of primary dendrites per cell (Fig. 4G,H). By contrast, Sema3d enhances significantly the percentage of RGCs with branches (Fig. 4I), whereas the number of dendrite branch points increases significantly in the presence of either Sema3d or Sema3f (Fig. 4J). These data indicate that Sema3s can act directly on RGCs to affect dendrites.

Thus, it was important to investigate next whether in the polarized *in vivo* environment of the retinal neuroepithelium, ectopic Sema3s leads to unbiasing of dendrite-like projections. cDNA constructs for myc-tagged *sema3d* or *sema3f* were electroporated along with *CS2-gfp* into stage 28 eye primordia. *CS2-sema3a-mt* was tested in a complementary set of experiments. Of note, myc immunoreactivity of the Sema3 proteins is essentially coincident with the GFP epifluorescence (Fig. 5E,F). We focused our analysis on *sema3*-transfected RGCs, postulating that high levels of secreted Sema3 would arise around these cells, and prevent them from capturing information about

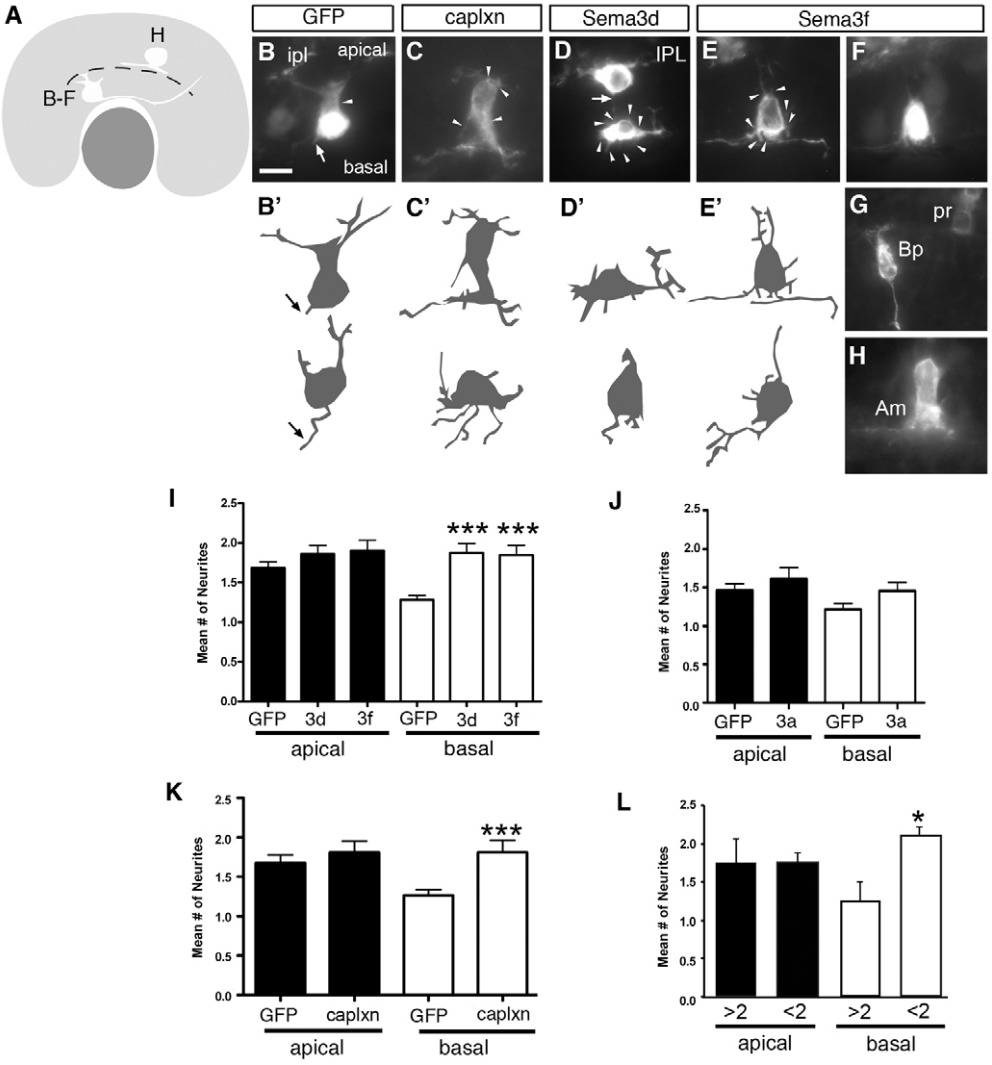

Fig. 5. Sema3 overexpression disrupts RGC dendrite polarization. (**A**) Schematic of a stage 39 retina with a representative RGC and amacrine cell to indicate the retinal location and orientation of the photomicrographs shown in B-F and H, respectively. (**B-F**) Stage 39 RGCs expressing different transgenes. GFP fluorescence is shown in B and F, and myc immunoreactivity in C-E. F is the GFP fluorescence of the myc-positive cell in E. Drawings of the cells in B-E, along with additional RGC examples, to capture the scope of phenotypes, are shown in B′-E′. Arrows show the axons, and arrowheads, dendrite-like neurites. ipl/IPL, inner plexiform layer. Scale bar: 10 μm. (**G**,**H**) A Sema3f-expressing photoreceptor (pr), bipolar cell (Bp) and amacrine cell (Am). Scale bar: in B, 15 μm for G; in B, 10 μm for H. (**I-K**) Graphs showing the mean number of apically or basally oriented neurites for RGCs overexpressing Sema3d/f (I), Sema3a (J) or caplxna1 (K). For I, GFP *n*=155, Sema3d *n*=80, Sema3f *n*=72. For J, GFP *n*=64, Sema3a *n*=54. For K, GFP *n*=98, caplxna1 *n*=58. (**L**) Graph showing the mean number of apically or basally oriented neurites for GFP-positive RGCs nearer than (<2; *n*=48) or farther than (>2; *n*=8) two cell body diameters from a myc-positive/Sema3f positive cell. Error bars represent s.e.m. Statistical significance in I was determined using a Kruskal–Wallis non-parametric one-way ANOVA, followed by a Dunn's multiple comparison test (***P<0.001), in J and K by a non-parametric Mann–Whitney U test (***P<0.001), and in L by a two-tailed, unpaired Student's *t*-test (*P<0.05). Data were collected from two to four independent experiments.

the Sema3 signals in the retina, which exhibit spatially restricted expression patterns. Many RGCs that ectopically express Sema3d or Sema3f fail to acquire a polarized morphology (Fig. 5D-F,D′,E′), exhibiting several basal neurites similar in appearance to the dendrite-like processes produced by dnnrp1-expressing RGCs. By contrast, control GFP-expressing RGCs exhibit a basal axon and apical dendrites (Fig. 5B,B′). Whereas a minority of control RGCs have more than one basal neurite at stage 39 (23.8%, *n*=155), this is true of the majority of Sema3d- (61.2%, *n*=80) and Sema3f- (61.1%, *n*=72) expressing RGCs. Indeed, Sema3d or Sema3f misexpression increases significantly the number of basal, but not apically oriented, neurites (Fig. 5I). By contrast, RGCs misexpressing Sema3a show a distribution of basal and apical neurites comparable to that observed in control RGCs (Fig. 5J). We verified that the Sema3a produced by our construct is functional by showing that Sema3a expressed by electroporated forebrain cells repels RGC axons (data not shown). Interestingly, RGCs that abut the inner plexiform layer are generally less affected than more basally located RGCs (Fig. 5D), possibly reflecting their ability to use non-Sema3-dependent cues arising from the inner plexiform layer or inner nuclear layer cells to polarize their dendrites. Of note, the polarized morphology of other retinal cell types, including bipolar and amacrine cells, is not obviously disrupted by Sema3 overexpression (Fig. 5G,H).

If dendrite polarization of Sema3-expressing RGCs is impaired because of Sema3 being secreted and disrupting endogenous Sema3 signals, then neighboring non-expressing RGCs should be similarly affected if they are sufficiently close. We assessed dendrite polarization of GFP-positive/Sema3f-negative (i.e. myc-negative) RGCs that were less than two cell diameters away from a Sema3f-positive (i.e. myc-positive) RGC and found a loss of apical bias of dendrite-like processes (Fig. 5L). This was not true for RGCs that were sufficiently far away (more than two cell diameters) from a Sema3f-expressing cell (Fig. 5L).

We next investigated whether the dendrite polarization phenotype generated with ectopic Sema3s results from excess Plxn signaling. To do so, we expressed in RGCs a constitutively active form of a Plxna1 receptor (*CS2-caplxna1-mt*), missing the SEMA domain that prevents Plxna1 activation in the basal state (Takahashi and Strittmatter, 2001). Similar to what is observed with ectopic Sema3 expression, an absence of apical bias of neurites occurs with RGCs expressing caplxna1 (Fig. 5C,C′): 22.7% (*n*=97) of GFP-expressing and 56.1% (*n*=58) of caplxna1-expressing cells have more than one basal neurite, and excess Plxna1 signaling increases the number of basally oriented neurites (Fig. 5K). Taken together, these data argue that Plxna1 signaling acts cell autonomously in RGCs to influence the polarization of RGC dendrites, and points to a Sema3 as the ligand(s) involved.

sema3f and *sema3a* are expressed in areas adjacent to RGCs at the time they initiate dendrites. To address whether Sema3f promotes proper polarization of RGC dendrites, we used an antisense (AS) oligonucleotide approach to knockdown Sema3f in the retina over the period of RGC dendritogenesis. AS-*sema3f* and *CS2-gfp* were co-electroporated at stage 27 into the eye, and embryos fixed at stage 39 for dendrite analysis. A sense *sema3a* oligonucleotide was used as control. Of note, because we have poor targeting of lens tissue by electroporation we could not test a requirement for Sema3a in RGC dendrite development. The total numbers of neurites are higher with knockdown of Sema3f than in control [control, 2.66±0.08 (s.e.m.) *n*=235 cells; AS-*sema3f*, 3.63±0.1 *n*=179 cells; *N*=3 independent experiments, $P<0.001$ unpaired Student's *t*-test], as are the numbers of basally oriented neurites [control, 1.26±0.04 (s.e.m.) *n*=233; AS-*sema3f*, 1.94±0.08 *n*=173; *N*=3 independent experiments, $P<0.001$ Mann–Whitney U test). These data argue that Sema3f is a ligand for Nrp1 in controlling RGC dendrite polarization.

DISCUSSION

Neurons are polarized structures and acquire asymmetry early on. We show that signal(s) acting through Nrp1 and Plxna1 ensures that dendrites are biased towards the apical side of the RGC. Disrupting the signaling through either Nrp1 or Plxna1 blocks the apical biasing of RGC dendritic projections. Several of the known ligands for these receptors, members of the Sema3 family, are expressed in the retina as RGC dendrites emerge. Sema3d and Sema3f can act directly on the dendrites of isolated RGCs, and *in vivo* Sema3f knockdown and Sema3 misexpression disrupt dendrite polarization. Taken together, these data identify Nrp1 and Plxna1 as mediating an extrinsic signal required for dendrite polarization, with one or more Sema3s as likely candidates.

Real-time imaging of zebrafish RGCs reveals that the dendrites initially project from random points around the cell (Choi et al., 2010). Subsequently, basal extensions are eliminated whereas apical dendrites continue to be elaborated. In *Xenopus*, from the start, however, projections are more common from the apical surface, and basal neurites are mostly absent by the time axons have reached the optic tract (Holt, 1989). Our data indicate that impairing the function of Nrp1 or Plxna1 results in more basally, but not apically, oriented neurites, which remain well after the axon reaches the optic tectum. These basal neurites are likely to be dendritic in nature. Morphologically they resemble dendrites, and for many transfected RGCs the basal dendrite-like neurites are clearly distinguishable from the thin, axon extending down to and along the retina's vitreal surface. When examined for dnnrp-expressing RGCs, the predicted axon is labeled with the axonal marker SMI-31, whereas the thick, short dendrite-like neurites are SMI-31 negative. Thus, our data argue that dendrite projections are biased towards the apical surface via an Nrp1/Plxna1-dependent mechanism. An alternative possibility is that basal dendrites simply fail to disappear when Nrp1/Plnxa1 signaling is impaired. We suggest that this explanation is less likely given that basal dendrites are not a predominant feature of *Xenopus* RGCs (Holt, 1989), dnnrp-expressing RGCs continue to develop normally (e.g. their axons extend to the optic tectum), and Sema3s are known for their roles in providing cells with spatial and directional information. RGCs in rat and zebrafish also express Nrp1 and Plxna receptors (de Winter et al., 2004; Liu et al., 2004), indicating that these receptors might control RGC dendrite development in other species.

For several reasons we argue that Nrp1 and Plxna1 transduce a Sema3 signal to promote apical polarization of dendrites. First, *plxna1*, *nrp1* and *sema3* expression initiate as dendrites emerge from RGCs. Second, the truncated Nrp1 and Plxna1 (Campbell et al., 2001; Takahashi et al., 1999; Tamagnone et al., 1999) both cause the emergence of basal neurites (Takahashi et al., 1999). Although it is possible that Plxna1 controls dendrite polarization by interacting with molecules other than Sema3s (Zhou et al., 2008), we observe the same polarization phenotype with blockade of Nrp1. Because Nrp1 and Plxna1 interact as a holoreceptor to mediate Sema3 signaling (Zhou et al., 2008), the simplest explanation for why the truncated Nrp1 and Plxna1 receptors produce similar dendrite phenotypes is that they cooperate to mediate a Sema3 signal. Third, disrupting a potential Sema3 signal through a Sema3 overexpression approach also disturbs dendrite polarization. Finally, knockdown of Sema3f expression in the

retina similarly promotes basal neurites. The fact that disrupted dendrite orientation is seen in RGCs with impaired Nrp1/Plxna1 receptor function is most readily explained if signaling through the complex itself alters dendrite polarization. It is possible, however, that Plxna1 signaling indirectly changes the responsiveness of RGCs to other environmental cues. For instance, Sema3f interferes with the growth-promoting effects of nerve growth factor on rat sympathetic neurons (Atwal et al., 2003). Yet, we find that Sema3d/f directly influences *Xenopus* RGC dendrite branching in culture, where presumably additional factors are either absent or present in limited amounts. Recent data in mouse indicate that transmembrane Sema receptors control RGC dendrite growth and targeting (Matsuoka et al., 2011a; Matsuoka et al., 2011b); thus, multiple Sema receptors from distinct families might coordinate the morphogenetic events that underlie proper formation of synaptic connections by RGCs.

The observation that activation of Plxna1 signaling, either through Sema3 overexpression or the caplxna1, generates similar unbiased neurite extensions as blocking Plxna1 signaling with the truncated Nrp1 and Plxna1 receptors is revealing. These data argue, but do not prove, that the spatial pattern of the input is important. Any disruption of the ability of RGCs to sense the pattern results in unbiased growth of dendrites from the soma. In this regard, Sema3s are interesting in that they expressed in a distributed fashion in the embryonic *Xenopus* retina. *sema3a* is present in the lens, on the basal side of the RGCs, whereas *sema3f* is present apical to the RGCs, in the adjacent cells of the inner nuclear layer. Our data best fit a model in which a spatially localized Sema3 is read by the developing RGC to provide information about which side of the cell is apical (Fig. 6). In culture, uniform application of Sema3s neither affects the numbers of primary neurites, nor pushes RGCs towards the polarized phenotype of their *in vivo* counterparts (axons and dendrites present on opposite sides of the cell). The fact that RGCs expressing mutant Sema3 receptors still initiate dendrites, just not in an apically biased fashion, indicates that Sema3s do not simply promote dendrite growth, but instead bias it to one side of the RGC, potentially by causing an asymmetric distribution of an intrinsic determinant (Barnes and Polleux, 2009). A direct effect of Sema3s on dendrite polarization seems likely, given their known guidance role and polarized expression pattern relative to the RGC; however, we cannot rule out the possibility that Sema3s act permissively to allow the expression of a pre-existing intrinsic polarity of the RGCs. The disruption of apical biasing of dendrites by ectopically expressed Sema3s argues against the latter; however, permissive effects could depend on a specific level of Sema3.

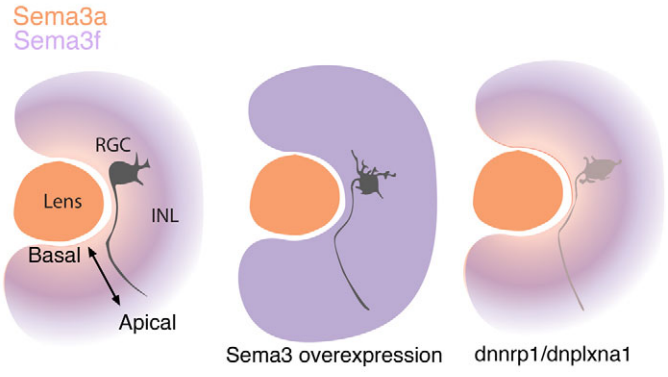

Fig. 6. Model of Nrp1 and Plxna1 function in dendrite polarization of RGCs. Schematic of the retina, and hypothesized gradients of Sema3a and Sema3f emanating from the lens and inner nuclear layer (INL), respectively. When these gradients are disrupted, by Sema3 overexpression or when RGCs expressing mutant Sema3 receptors are unable to sense the Sema3 gradients, RGC dendrites fail to polarize towards the apical surface of the cell.

Sema3f appears to function in dendrite polarization, with knockdown of Sema3f disrupting the event. The secreted Sema3f protein could be present at higher levels apically than basally, promoting the emergence of apical dendrites at the expense of basal ones. Sema3f has a considerably higher binding affinity for Nrp2 than for Nrp1 (Chen et al., 1997), but our data indicate that *nrp2* is not expressed by early differentiating RGCs. Because both Sema3f and Nrp1 manipulations similarly affect RGC dendrite polarization, a non Nrp-dependent mechanism seems doubtful (Steinbach et al., 2002). More likely, given that the binding affinity of Sema3f for Nrp1 is similar to that of Sema3a (Chen et al., 1997), is that Sema3f might function through Nrp1 if Nrp2 is not present. Carboxy terminal proteolytic processing of Sema3f could further enhance binding of Sema3f to Nrp1 (Parker et al., 2010). Whether other Sema3s also participate in dendrite polarization is unclear. Although Sema3a might function via Nrp1 to polarize embryonic mouse cortical neurons (Shelly et al., 2011), Sema3a has no significant effect on *Xenopus* RGC dendrites *in vitro* or *in vivo*. Sema3d also seems an unlikely candidate in that it is expressed by cells in the ciliary marginal zone of the peripheral retina, distant from the differentiating RGCs.

Our model for Nrp1 involvement in RGC dendrite polarization is in contrast to how Nrp1/Sema3a is suggested to function in neuronal polarization of mouse hippocampal neurons and *Xenopus* spinal cord interneurons (Nishiyama et al., 2011; Shelly et al., 2011). For these two neuronal types, Sema3a promotes neuronal polarization by suppressing axon growth. For hippocampal neurons, dendrite growth probably becomes polarized secondary to axonal suppression (an event that is impaired by siRNA for Nrp1), whereas Sema3a directly promotes dendrite characteristics at the expense of an axonal phenotype for the spinal interneurons. By contrast, for RGCs, axons emerge and extend out of the eye prior to dendrite initiation, and although blockade of Nrp1/Plxna1 affects RGC dendrite polarization, RGC axons appear to be unperturbed (though the truncated receptors are present as RGC axons emerge). Indeed, this receptor signaling pathway is only switched on in RGCs after their axons have left the retina. For hippocampal and spinal cord neurons, dendrite polarization is promoted through suppression of axon growth, yet in our system *sema3a*-expressing lens cells are adjacent to the vitreal surface over which RGC axons extend, and furthest away from the apical surface from which the dendrites emerge. Thus, Nrp1-dependent polarization of *Xenopus* RGC dendrites occurs via a different scenario, apparently axon independent, than that observed for these other neuron types.

Our data indicate that receptors for a member of a classical axon guidance molecule family, the class III semaphorins, provide an axon-independent means to polarize the growth of RGC dendrites. Appealingly, careful temporal regulation of the expression of the receptors by the RGC helps separate roles for the same Nrp1 receptor in both axon guidance and dendrite polarization. Most axons have left the retina by the time they express Nrp1/Plxna1, and so the ligand that acts on these receptors affects only the morphogenesis of the RGC dendrites. Given that Nrp1 helps promote RGC dendrite growth and yet supports RGC axon repulsion, it is likely that the signaling downstream of Nrp1 in the two morphogenetic events differs.

Acknowledgements
We thank Drs K. Atkinson-Leadbeater, J. S. Bains, D. Kurrasch and C. Schuurmans for helpful comments on the manuscript. Drs Strittmatter and Tamagnone kindly provided cDNA constructs.

Funding
E.M.K. was supported by the Foundation for Fighting Blindness and by the Alberta Heritage Foundation for Medical Research (AHFMR). S.M. is an AHFMR Scientist and a Tier II Canada Research Chair in Developmental Neurobiology. The work was supported by an operating grant from the Canadian Institutes of Health Research to S.M.

Competing interests statement
The authors declare no competing financial interests.

Author contributions
E.M.K. generated and analyzed the data in Figs 1 and 3 and some data for Fig. 2. C.L.H. generated selected data for Fig. 2 and all of the data for Figs 4 and 5. J.J. aided data collection and generated the dnnrp1 construct. G.E.B. identified the various Sema3 genes and *nrp1* and *nrp2*. S.M. analyzed the data for Figs 2, 4 and 5, generated all figures and wrote the manuscript. All authors helped in editing the manuscript.

Supplementary material
Supplementary material available online at
http://dev.biologists.org/lookup/suppl/doi:10.1242/dev.088286/-/DC1

References
Arimura, N. and Kaibuchi, K. (2007). Neuronal polarity: from extracellular signals to intracellular mechanisms. *Nat. Rev. Neurosci.* **8**, 194-205.
Atkinson-Leadbeater, K., Bertolesi, G. E., Hehr, C. L., Webber, C. A., Cechmanek, P. B. and McFarlane, S. (2010). Dynamic expression of axon guidance cues required for optic tract development is controlled by fibroblast growth factor signaling. *J. Neurosci.* **30**, 685-693.
Atwal, J. K., Singh, K. K., Tessier-Lavigne, M., Miller, F. D. and Kaplan, D. R. (2003). Semaphorin 3F antagonizes neurotrophin-induced phosphatidylinositol 3-kinase and mitogen-activated protein kinase kinase signaling: a mechanism for growth cone collapse. *J. Neurosci.* **23**, 7602-7609.
Barnes, A. P. and Polleux, F. (2009). Establishment of axon-dendrite polarity in developing neurons. *Annu. Rev. Neurosci.* **32**, 347-381.
Callander, D. C., Lamont, R. E., Childs, S. J. and McFarlane, S. (2007). Expression of multiple class three semaphorins in the retina and along the path of zebrafish retinal axons. *Dev. Dyn.* **236**, 2918-2924.
Campbell, D. S., Regan, A. G., Lopez, J. S., Tannahill, D., Harris, W. A. and Holt, C. E. (2001). Semaphorin 3A elicits stage-dependent collapse, turning, and branching in Xenopus retinal growth cones. *J. Neurosci.* **21**, 8538-8547.
Chen, H., Chédotal, A., He, Z., Goodman, C. S. and Tessier-Lavigne, M. (1997). Neuropilin-2, a novel member of the neuropilin family, is a high affinity receptor for the semaphorins Sema E and Sema IV but not Sema III. *Neuron* **19**, 547-559.
Choi, J. H., Law, M. Y., Chien, C. B., Link, B. A. and Wong, R. O. (2010). In vivo development of dendritic orientation in wild-type and mislocalized retinal ganglion cells. *Neural Dev.* **5**, 29.
de Winter, F., Cui, Q., Symons, N., Verhaagen, J. and Harvey, A. R. (2004). Expression of class-3 semaphorins and their receptors in the neonatal and adult rat retina. *Invest. Ophthalmol. Vis. Sci.* **45**, 4554-4562.
Gonthier, B., Koncina, E., Satkauskas, S., Perraut, M., Roussel, G., Aunis, D., Kapfhammer, J. P. and Bagnard, D. (2009). A PKC-dependent recruitment of MMP-2 controls semaphorin-3A growth-promoting effect in cortical dendrites. *PLoS ONE* **4**, e5099.
Hocking, J. C., Hehr, C. L., Bertolesi, G. E., Wu, J. Y. and McFarlane, S. (2010). Distinct roles for Robo2 in the regulation of axon and dendrite growth by retinal ganglion cells. *Mech. Dev.* **127**, 36-48.
Hocking, J. C., Hehr, C. L., Chang, R. Y., Johnston, J. and McFarlane, S. (2008). TGFbeta ligands promote the initiation of retinal ganglion cell dendrites in vitro and in vivo. *Mol. Cell. Neurosci.* **37**, 247-260.
Holt, C. E. (1989). A single-cell analysis of early retinal ganglion cell differentiation in Xenopus: from soma to axon tip. *J. Neurosci.* **9**, 3123-3145.
Kim, S. and Chiba, A. (2004). Dendritic guidance. *Trends Neurosci.* **27**, 194-202.
Koestner, U., Shnitsar, I., Linnemannstöns, K., Hufton, A. L. and Borchers, A. (2008). Semaphorin and neuropilin expression during early morphogenesis of Xenopus laevis. *Dev. Dyn.* **237**, 3853-3863.
Koncina, E., Roth, L., Gonthier, B. and Bagnard, D. (2007). Role of semaphorins during axon growth and guidance. *Adv. Exp. Med. Biol.* **621**, 50-64.
Liu, Y., Berndt, J., Su, F., Tawarayama, H., Shoji, W., Kuwada, J. Y. and Halloran, M. C. (2004). Semaphorin3D guides retinal axons along the dorsoventral axis of the tectum. *J. Neurosci.* **24**, 310-318.
Matsuoka, R. L., Chivatakarn, O., Badea, T. C., Samuels, I. S., Cahill, H., Katayama, K., Kumar, S. R., Suto, F., Chédotal, A., Peachey, N. S. et al. (2011a). Class 5 transmembrane semaphorins control selective mammalian retinal lamination and function. *Neuron* **71**, 460-473.
Matsuoka, R. L., Nguyen-Ba-Charvet, K. T., Parray, A., Badea, T. C., Chédotal, A. and Kolodkin, A. L. (2011b). Transmembrane semaphorin signalling controls laminar stratification in the mammalian retina. *Nature* **470**, 259-263.
McFarlane, S. and Lom, B. (2012). The Xenopus retinal ganglion cell as a model neuron to study the establishment of neuronal connectivity. *Dev. Neurobiol.* **72**, 520-536.
McFarlane, S., McNeill, L. and Holt, C. E. (1995). FGF signaling and target recognition in the developing Xenopus visual system. *Neuron* **15**, 1017-1028.
Morita, A., Yamashita, N., Sasaki, Y., Uchida, Y., Nakajima, O., Nakamura, F., Yagi, T., Taniguchi, M., Usui, H., Katoh-Semba, R. et al. (2006). Regulation of dendritic branching and spine maturation by semaphorin3A-Fyn signaling. *J. Neurosci.* **26**, 2971-2980.
Nakamura, F. and Goshima, Y. (2002). Structural and functional relation of neuropilins. *Adv. Exp. Med. Biol.* **515**, 55-69.
Nieuwkoop, P. D. and Faber, J. (1994). *Normal Table of Xenopus Laevis*. New York, NY: Garland.
Nishiyama, M., Togashi, K., von Schimmelmann, M. J., Lim, C. S., Maeda, S., Yamashita, N., Goshima, Y., Ishii, S. and Hong, K. (2011). Semaphorin 3A induces CaV2.3 channel-dependent conversion of axons to dendrites. *Nat. Cell Biol.* **13**, 676-685.
Ohta, K., Takagi, S., Asou, H. and Fujisawa, H. (1992). Involvement of neuronal cell surface molecule B2 in the formation of retinal plexiform layers. *Neuron* **9**, 151-161.
Parker, M. W., Hellman, L. M., Xu, P., Fried, M. G. and Vander Kooi, C. W. (2010). Furin processing of semaphorin 3F determines its anti-angiogenic activity by regulating direct binding and competition for neuropilin. *Biochemistry* **49**, 4068-4075.
Polleux, F., Morrow, T. and Ghosh, A. (2000). Semaphorin 3A is a chemoattractant for cortical apical dendrites. *Nature* **404**, 567-573.
Randlett, O., Norden, C. and Harris, W. A. (2011). The vertebrate retina: a model for neuronal polarization in vivo. *Dev. Neurobiol.* **71**, 567-583.
Renzi, M. J., Feiner, L., Koppel, A. M. and Raper, J. A. (1999). A dominant negative receptor for specific secreted semaphorins is generated by deleting an extracellular domain from neuropilin-1. *J. Neurosci.* **19**, 7870-7880.
Schlomann, U., Schwamborn, J. C., Müller, M., Fässler, R. and Püschel, A. W. (2009). The stimulation of dendrite growth by Sema3A requires integrin engagement and focal adhesion kinase. *J. Cell Sci.* **122**, 2034-2042.
Shelly, M., Cancedda, L., Lim, B. K., Popescu, A. T., Cheng, P. L., Gao, H. and Poo, M. M. (2011). Semaphorin3A regulates neuronal polarization by suppressing axon formation and promoting dendrite growth. *Neuron* **71**, 433-446.
Sive, H. L., Grainger, R. M. and Harland, R. M. (2000). *Early Development of Xenopus Laevis: A Laboratory Manual*. Cold Spring Harbor, NY: Cold Spring Harbor Laboratory Press.
Sokal, R. R. and Rohlf, F. J. (2011). *Biometry: The Principles and Practices of Statistics in Biological Research*. New York, NY: Freeman.
Steinbach, K., Volkmer, H. and Schlosshauer, B. (2002). Semaphorin 3E/collapsin-5 inhibits growing retinal axons. *Exp. Cell Res.* **279**, 52-61.
Tahirovic, S. and Bradke, F. (2009). Neuronal polarity. *Cold Spring Harb. Perspect. Biol.* **1**, a001644.
Takagi, S., Hirata, T., Agata, K., Mochii, M., Eguchi, G. and Fujisawa, H. (1991). The A5 antigen, a candidate for the neuronal recognition molecule, has homologies to complement components and coagulation factors. *Neuron* **7**, 295-307.
Takahashi, T., Fournier, A., Nakamura, F., Wang, L. H., Murakami, Y., Kalb, R. G., Fujisawa, H. and Strittmatter, S. M. (1999). Plexin-neuropilin-1 complexes form functional semaphorin-3A receptors. *Cell* **99**, 59-69.
Takahashi, T. and Strittmatter, S. M. (2001). Plexina1 autoinhibition by the plexin sema domain. *Neuron* **29**, 429-439.
Tamagnone, L., Artigiani, S., Chen, H., He, Z., Ming, G. I., Song, H., Chedotal, A., Winberg, M. L., Goodman, C. S., Poo, M. et al. (1999). Plexins are a large family of receptors for transmembrane, secreted, and GPI-anchored semaphorins in vertebrates. *Cell* **99**, 71-80.
Togashi, K., von Schimmelman, M. J., Nishiyama, M., Lim, C. S., Yoshkida, N., Yun, B., Molday, R. S., Goshima, Y. and Hong, K. (2008). Cyclic GMP-gated CNG channels function in Sema3A-induced growth cone repulsion. *Neuron* **58**, 694-707.
Zhou, Y., Gunput, R. A. and Pasterkamp, R. J. (2008). Semaphorin signaling: progress made and promises ahead. *Trends Biochem. Sci.* **33**, 161-170.

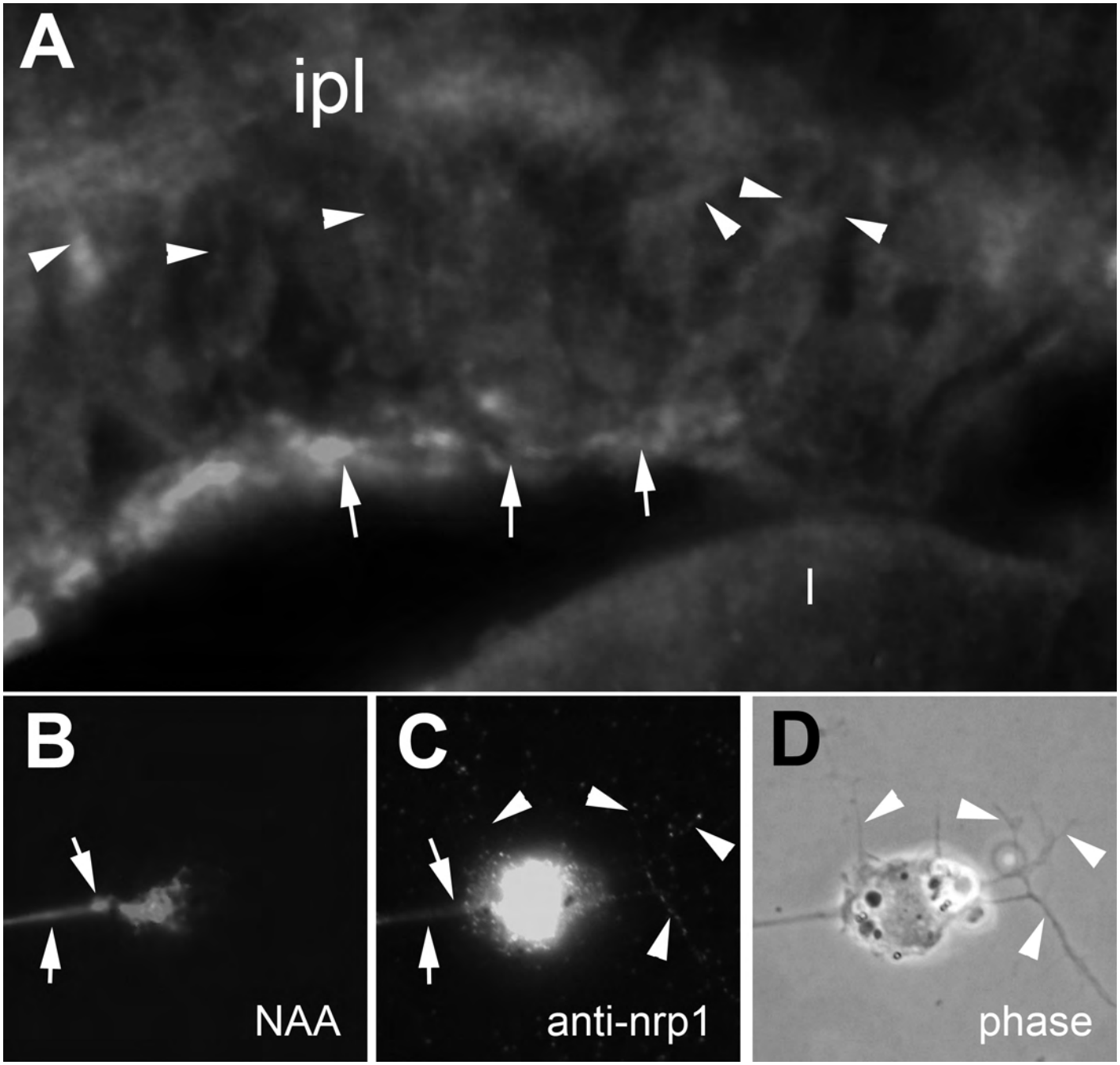

Fig. S1. Nrp1 expressed in the dendrites of developing RGCs. (**A**) An antibody against Nrp1 shows Nrp1-like immunoreactivity in the dendrites of developing RGCs (arrowheads) and their axons (arrows). (**B-D**) Isolated NAA-positive RGC in dissociated retinal culture shows NAA immunoreactivity in its axon (arrow) but not in its dendrites (arrowheads) (B), whereas the antibody against Nrp1 (C) labels both the axon and the dendrites. The same RGC is shown in phase in D. ipl, inner plexiform layer; l, lens.